AMERICAN SOCIETY FOR MICROBIOLOGY | Applied and Environmental Microbiology®

MICROBIAL ECOLOGY

Cooccurring Activities of Two Autotrophic Pathways in Symbionts of the Hydrothermal Vent Tubeworm *Riftia pachyptila*

Juliana M. Leonard,[a] Jessica Mitchell,[b] Roxanne A. Beinart,[c] Jennifer A. Delaney,[b] Jon G. Sanders,[b] Greg Ellis,[d] Ethan A. Goddard,[d] Peter R. Girguis,[b] Kathleen M. Scott[a]

[a]Department of Integrative Biology, University of South Florida, Tampa, Florida, USA
[b]Department of Organismic and Evolutionary Biology, Harvard University, Cambridge, Massachusetts, USA
[c]Graduate School of Oceanography, University of Rhode Island, Narragansett, Rhode Island, USA
[d]College of Marine Science, University of South Florida, St. Petersburg, Florida, USA

ABSTRACT Genome and proteome data predict the presence of both the reductive citric acid cycle (rCAC; also called the reductive tricarboxylic acid cycle) and the Calvin-Benson-Bassham cycle (CBB) in "*Candidatus* Endoriftia persephonae," the autotrophic sulfur-oxidizing bacterial endosymbiont from the giant hydrothermal vent tubeworm *Riftia pachyptila*. We tested whether these cycles were differentially induced by sulfide supply, since the synthesis of biosynthetic intermediates by the rCAC is less energetically expensive than that by the CBB. *R. pachyptila* was incubated under *in situ* conditions in high-pressure aquaria under low (28 to 40 μmol · h^{-1}) or high (180 to 276 μmol · h^{-1}) rates of sulfide supply. Symbiont-bearing trophosome samples excised from *R. pachyptila* maintained under the two conditions were capable of similar rates of CO_2 fixation. Activities of the rCAC enzyme ATP-dependent citrate lyase (ACL) and the CBB enzyme 1,3-bisphosphate carboxylase/oxygenase (RubisCO) did not differ between the two conditions, although transcript abundances for ATP-dependent citrate lyase were 4- to 5-fold higher under low-sulfide conditions. $\delta^{13}C$ values of internal dissolved inorganic carbon (DIC) pools were varied and did not correlate with sulfide supply rate. In samples taken from freshly collected *R. pachyptila*, $\delta^{13}C$ values of lipids fell between those collected for organisms using either the rCAC or the CBB exclusively. These observations are consistent with cooccurring activities of the rCAC and the CBB in this symbiosis.

IMPORTANCE Previous to this study, the activities of the rCAC and CBB in *R. pachyptila* had largely been inferred from "omics" studies of *R. pachyptila* without direct assessment of *in situ* conditions prior to collection. In this study, *R. pachyptila* was maintained and monitored in high-pressure aquaria prior to measuring its CO_2 fixation parameters. Results suggest that ranges in sulfide concentrations similar to those experienced *in situ* do not exert a strong influence on the relative activities of the rCAC and the CBB. This observation highlights the importance of further study of this symbiosis and other organisms with multiple CO_2-fixing pathways, which recent genomics and biochemical studies suggest are likely to be more prevalent than anticipated.

KEYWORDS CO_2 fixation, reductive citric acid cycle, Calvin-Benson-Bassham cycle, hydrothermal vent, *Riftia pachyptila*, *Candidatus* Endoriftia persephonae, carbon dioxide fixation

Vestimentiferan tubeworms are often the dominant macrofauna at deep-sea hydrothermal vents and cold seeps (1). Bushes of these bacteria-invertebrate symbioses flourish in sulfidic deep-sea habitats (2, 3). Numerous organisms either consume them

Citation Leonard JM, Mitchell J, Beinart RA, Delaney JA, Sanders JG, Ellis G, Goddard EA, Girguis PR, Scott KM. 2021. Cooccurring activities of two autotrophic pathways in symbionts of the hydrothermal vent tubeworm *Riftia pachyptila*. Appl Environ Microbiol 87:e00794-21. https://doi.org/10.1128/AEM.00794-21.

Editor Haruyuki Atomi, Kyoto University

Address correspondence to Kathleen M. Scott, kmscott@usf.edu.

Received 23 April 2021
Accepted 22 June 2021
Accepted manuscript posted online 30 June 2021
Published 11 August 2021

or live among their tubes; vestimentiferan tubeworms function as ecosystem-structuring primary producers (4, 5).

These chemolithoautotrophic symbioses obtain organic carbon via CO_2 fixation by intracellular sulfur-oxidizing autotrophic bacteria ("*Candidatus* Endoriftia persephonae" [6–9]). The sulfide ($\sum H_2S$; = H_2S + HS^- + S^{2-}), O_2, and CO_2 needed for chemolithoautotrophy are absorbed by the plume, an anterior gas exchange organ (10). As the gases dissolve into the tubeworm's blood, they are bound by extracellular hemoglobins, which deliver them to the trophosome, a well-vascularized organ that fills the body cavity and is comprised primarily of bacteriocytes that house the endosymbionts (11, 12). The endosymbionts use sulfur oxidation to power CO_2 fixation, and the host tubeworm assimilates organic carbon from the endosymbionts (9, 13, 14).

One unusual aspect of tubeworm endosymbiont physiology is the presence of two pathways for autotrophic CO_2 fixation. "Omics," enzyme, and stable isotope data all provide evidence for the operation of both the Calvin-Benson-Bassham cycle (CBB) and the reductive citric acid cycle (rCAC) in these organisms (15–19). Autotrophic microorganisms typically rely on a single pathway for CO_2 fixation, but genome studies are revealing several with the genetic potential to use two pathways (19–21), which challenges the current understanding of the ecophysiology of CO_2 fixation. Why or how both pathways would operate in a single organism is not clear; among other factors, the rCAC and CBB have very different tolerances for O_2, with the CBB being generally more robust to the presence of this dissolved gas (22) (but see Lücker et al. [23]). Since biomass synthesis via the CBB is more energetically expensive than that via the rCAC (24), it has been suggested that the endosymbionts might differentially regulate the pathways based on $\sum H_2S$ availability in their habitat. It has been proposed that the rCAC could predominate when $\sum H_2S$ is scarce, while the CBB could be used when $\sum H_2S$ is more abundant (15).

This hypothesis is particularly compelling when considering hydrothermal vent tubeworms such as *Riftia pachyptila*, since $\sum H_2S$ concentrations in their habitat can be quite erratic (25). At vents, $\sum H_2S$ is supplied from dilute hydrothermal fluid emitted from cracks in the basalt substratum. As this warm (2 to 40°C), anoxic fluid meets cold (2°C) bottom seawater, eddies are formed. As a result, *R. pachyptila* bushes are subject to seconds- to days-long oscillations in $\sum H_2S$ (0 to 725 μM) and O_2 (0 to100 μM) (17, 26, 27).

R. pachyptila has adaptations to maintain a steady supply of $\sum H_2S$ and O_2 to the symbionts despite the environmental heterogeneity. The hemoglobin-containing blood and coelomic fluids have a high capacity for both gases and likely dampen these oscillations in availability considerably (11, 28). However, longer-term changes in $\sum H_2S$ availability are likely to have an impact on the symbionts. *R. pachyptila* trophosomes differ considerably in hue, which is correlated with elemental sulfur content. Elemental sulfur is an intermediate in $\sum H_2S$ oxidation by "*Ca.* E. persephonae." Yellow or green trophosomes have a high elemental sulfur content, while black trophosomes have lower elemental sulfur content, due to depletion of stored elemental sulfur by the symbionts (29). *R. pachyptila* freshly collected from hydrothermal vents has trophosomes with a range of sulfur contents (30), and it has been inferred that trophosome color corresponds to the $\sum H_2S$ of the collection site; tubeworms with darker trophosomes are inferred to inhabit lower $\sum H_2S$ habitats, while those with lighter trophosomes are inferred to inhabit higher $\sum H_2S$ habitats (29). This range in sulfur contents suggests that long-term changes in external $\sum H_2S$ supply result in changes in the internal supply of reduced sulfur electron donors available to the symbionts, which are likely to elicit responses in symbiont physiology, including expression of CO_2-fixing pathways.

Thus far, the evidence is mixed for differential regulation of the rCAC and the CBB as a response to $\sum H_2S$ supply. Trophosome proteomes from freshly collected *R. pachyptila* with dark (low-sulfur) trophosomes sometimes show higher levels of rCAC-associated proteins compared to those of yellow or green (high-sulfur) trophosomes

(15, 31), but sometimes they do not (17, 32). Transcript abundances and proteome data from size-fractionated "*Ca.* E. persephonae" also do not suggest a clear pattern of differential regulation of the rCAC and the CBB in response to $\sum H_2S$ supply. Larger symbiont cells contain larger amounts of elemental sulfur, suggesting exposure to higher $\sum H_2S$ supply; if $\sum H_2S$ supply regulates the two carbon-fixing pathways, CBB enzymes should be more abundant in larger symbiont cells, while rCAC enzymes should be more abundant in smaller symbiont cells. Transcript abundances for *cbbM* (form II ribulose 1,3-bisphosphate carboxylase/oxygenase [RubisCO], EC 4.1.1.39; CBB), the sole RubisCO gene in the symbiont genome, are higher (~5-fold) in large symbionts, as is that of CbbM protein (1.8-fold higher), appearing to confirm a correlation between high $\sum H_2S$ supply and the CBB. However, transcript abundances of *aclB* (β subunit of ATP-dependent citrate lyase [ACL], EC 2.3.3.8; rCAC) are also higher (~1.4-fold) in large symbionts (32), as is that of AclA protein (α subunit of ACL; 1.8-fold higher). Oddly, the abundance of the AclB protein (β subunit of ACL) is 1.2-fold lower in these cells (32).

R. pachyptila biomass $\delta^{13}C$ values (= $[(R_{sample}/R_{std}) - 1]$, where $R_{sample} = {}^{13}C/{}^{12}C$ in a sample and $R_{std} = {}^{13}C/{}^{12}C$ in the Vienna Pee Dee Belemnite (VPDB) standard [33, 34]) suggest inputs from both the rCAC and the CBB. Provided that organisms are drawing from sources of environmental dissolved inorganic carbon (DIC; = $CO_2 + HCO_3^- + CO_3^{-2}$) with "typical" values of −1 to +1 ‰, as has been measured at the hydrothermal vents inhabited by *R. pachyptila* (35, 36), autotrophs using the rCAC typically have biomass $\delta^{13}C$ values of −9 to −13‰, while those using the CBB typically have values of −24 to −26‰ (37–43). $\delta^{13}C$ values for *R. pachyptila* are −9 to −16‰ (44). The $\delta^{13}C$ values of proteins from "*Ca.* E. persephonae" from dark trophosome samples are more ^{13}C-enriched than those from yellow or green trophosome samples, suggesting added input of carbon fixation via the rCAC in these symbionts (32). Lipid-specific $\delta^{13}C$ values can also provide evidence for the activities of rCAC and CBB. Autotrophic organisms using the CBB introduce carbon into glycolysis/gluconeogenesis, while those using the rCAC introduce carbon into the citric acid cycle (24). The acetyl-coenzyme A (CoA) needed to synthesize fatty acids to incorporate into cell membrane phospholipids is generated differently when organisms are using the CBB versus the rCAC. For organisms using the CBB, carbon is passed through the final reactions of glycolysis, and the pyruvate dehydrogenase complex (EC 1.2.4.1, 2.3.1.12, and 1.8.1.4) introduces it to the oxidative citric acid cycle to make precursor compounds for biosynthesis. Some of the acetyl-CoA produced by pyruvate dehydrogenase is used for fatty acid synthesis. Pyruvate dehydrogenase discriminates against ^{13}C (45) and, as a result, the acetyl moieties of the acetyl-CoA molecules that it synthesizes are enriched in ^{12}C, resulting in more negative $\delta^{13}C$ values for the lipids synthesized from this acetyl-CoA (46). For organisms using the rCAC, the acetyl-CoA needed for fatty acid synthesis is formed by ACL, and lipids in these organisms are not enriched in ^{12}C (46). As a result, lipid $\delta^{13}C$ values have been used to infer the activities of rCAC and CBB in autotrophic organisms (46); surprisingly, they have not been reported for *R. pachyptila*.

These previous studies relied on samples taken from *R. pachyptila* that had been freshly collected by submersible from the deep-sea hydrothermal vent environment, which has the potential to confound interpretation of resulting data. If *R. pachyptila* was gathered at the very end of the submersible dive, it had an hour-long transit to the surface (K. M. Scott, personal observation), followed by many hours in a cold room before dissection (31). The environmental conditions experienced by these worms was inferred indirectly via trophosome color, which is used as a proxy for environmental $\sum H_2S$ (15, 31, 32). Results from these studies may be compromised by changes in transcriptome and proteome that could occur between collection and analysis, as well as uncertainty about the conditions the organisms had experienced prior to collection.

This study was designed to address the hypothesis that the rCAC and the CBB are differentially regulated in response to $\sum H_2S$, using *R. pachyptila* individuals that were placed in high-pressure aquaria immediately upon recovery at the surface and

maintained at pressures, temperatures, and $\sum H_2S$ and O_2 concentrations spanning the range measured *in situ*. Conditions in high-pressure aquaria were monitored for 2 to 3 days, providing a measured history of $\sum H_2S$ exposure, and *R. pachyptila* samples were dissected immediately upon depressurization.

RESULTS

Comparison of parameters measured from *R. pachyptila* individuals maintained in aquaria with previously reported measurements. Physiological parameters measured from *R. pachyptila* individuals maintained in high-pressure aquaria are listed individually in Tables S1 to S3 in the supplemental material, and are similar to previously reported measurements. Concentrations of $\sum H_2S$ in mixtures of blood and coelomic fluid were 0.012 to 4.008 mM, overlapping with the range previously observed in *R. pachyptila* individuals maintained in high-pressure aquaria (blood and coelomic fluid $\sum H_2S$ to 10 mM [47]). Other parameters spanned the range observed in freshly collected *R. pachyptila* specimens. Trophosome sulfur content ranged from 3 to 22.6% (for freshly collected individuals, 0.4 to 10.3% [30]). Trophosome CO_2 fixation rates were 3.67 to 26.4 μmol · h^{-1} · g^{-1}, similar to those measured from freshly collected *R. pachyptila* samples and incubated under similar conditions (11 to 25 μmol · h^{-1} · g^{-1} [48]). Enzyme activities also matched previously measured values (RuBisCO, this study, 0.002 to 0.0117 μmol · min^{-1} · mg $protein^{-1}$; in previous studies, 0.006 to 0.029 μmol · min^{-1} · mg $protein^{-1}$ [49, 50]; ACL, this study, 0.04 to 0.459 μmol · min^{-1} · mg $protein^{-1}$; in a previous study, 0.032 μmol · min^{-1} · mg $protein^{-1}$ [15]). $\delta^{13}C$ values of biomass (−10.3 to −13.5‰) also resemble those previously collected from fresh individuals (−9 to −16‰ [51]).

Impact of $\sum H_2S$ supply on internal forms of sulfur in *R. pachyptila*. *R. pachyptila* individuals maintained in aquaria with low concentrations of $\sum H_2S$ due to low rates of $\sum H_2S$ supply (Fig. 1) had low $\sum H_2S$ concentrations in blood and coelomic fluid. *R. pachyptila* individuals incubated in aquaria with high concentrations of $\sum H_2S$ had higher $\sum H_2S$ concentrations in blood and coelomic fluid (Fig. 2A and Table 1, $P < 0.01$; see also Tables S1 and S2). Trophosome elemental sulfur content was often much higher in *R. pachyptila* individuals incubated under higher $\sum H_2S$ conditions (Fig. 2B), but the correlation between trophosome elemental sulfur content and aquarium $\sum H_2S$ concentration or supply was weaker (Table 1; $P = 0.079$ and 0.225, respectively). Trophosome elemental sulfur content did reflect the $\sum H_2S$ concentrations in blood and coelomic fluid (Table 1; $P = 0.014$).

Impact of $\sum H_2S$ and O_2 supply on symbiont CO_2 fixation parameters. Symbiont autotrophic potential, which was assayed by measuring the CO_2 fixation rate by trophosome samples that had been gently disrupted to keep the symbionts intact, did not reflect $\sum H_2S$ concentrations in, or rates of supply to, aquaria (Table 2 and Table S1). Trophosome CO_2 fixation rates also did not reflect the concentration of $\sum H_2S$ measured in the blood and coelomic fluid of the *R. pachyptila* individuals from which the trophosome samples had been excised, nor did they reflect the trophosome elemental sulfur content (Table 2).

Activities of ACL and RubisCO also did not correlate with $\sum H_2S$ abundance in the aquaria with or $\sum H_2S$ concentrations in blood and coelomic fluid (Table 2 and Fig. 3). The ACL assay detected similar levels of activity of this enzyme in both trophosome and vestimentum samples (see Table S4 in the supplemental material), which suggests that the ACL activities measured in the trophosome are a combination of host and symbiont enzyme activities.

$\Delta\delta^{13}C$ values, calculated from differences in $\Delta\delta^{13}C$ values of internal and external DIC (Tables S2 and S3), did not reflect internal or external $\sum H_2S$ abundance, or elemental sulfur content. If the rCAC predominates when reduced sulfur compounds are scarce, and the CBB predominates when they are more abundant, positive correlations are expected, as the CBB discriminates far more strongly against ^{13}C-DIC than the rCAC does (46). This should result in more positive $\delta^{13}C$ values for DIC in trophosome or blood and coelomic fluid samples compared to those for DIC in the aquarium water.

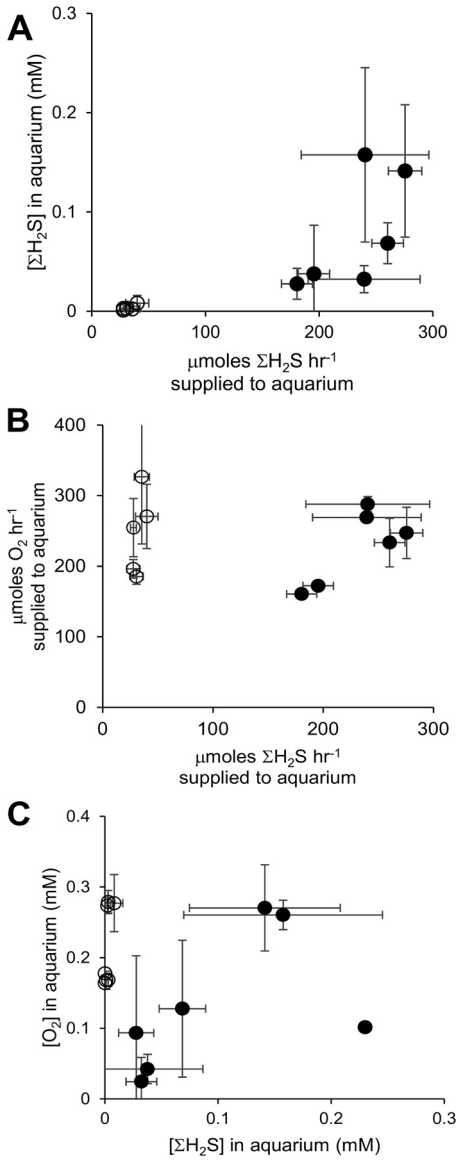

FIG 1 $\sum H_2S$ and oxygen concentrations in high-pressure flowthrough aquaria used to maintain *Riftia pachyptila*. (A) $\sum H_2S$ concentrations in the aquaria as a function of the rate of $\sum H_2S$ supply to the aquaria. (B) Rate of $\sum H_2S$ supply to the aquaria versus rate of supply of O_2. (C) O_2 concentrations versus $\sum H_2S$ concentrations in the aquaria. Open symbols indicate "low $\sum H_2S$" aquaria, and filled symbols indicate "high $\sum H_2S$" aquaria. Error bars indicate the standard deviations of the data.

Instead, some comparisons had positive correlations, others had negative correlations, and none of the models fitting the data were strongly supported (Table 2).

Likewise, there did not appear to be a connection between O_2 supply and symbiont CO_2 fixation parameters (Table 3). While $\Delta\delta^{13}C$ values regressed on O_2 supply sometimes resulted in models with strong support ($P = 0.008$ to 0.044; Table 3), one correlation was negative and two were positive, which does not provide support for rCAC or CBB activity responding to environmental O_2 concentrations.

Symbiont CO_2 fixation parameters did not correlate with each other (Table 4). Neither RubisCO nor ACL activity correlated with trophosome CO_2 fixation rates or with $\Delta\delta^{13}C$ values. However, ACL and RubisCO activity may be positively correlated ($P = 0.056$).

Impact of $\sum H_2S$ supply rate on transcription of genes encoding CBB and rCAC enzymes. Transcripts per million (tpm) of both subunits of ACL were more abundant under low $\sum H_2S$ conditions than under high $\sum H_2S$ conditions (Fig. 4; $P < 0.05$), with β values of 2.3 and 2.04 for the alpha and beta subunits of ACL. These values correspond

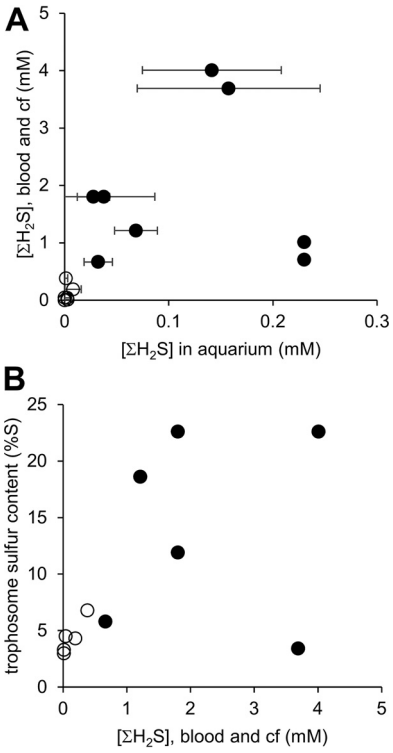

FIG 2 Internal and external sulfur parameters of *Riftia pachyptila* maintained in high-pressure flowthrough aquaria. (A) $\sum H_2S$ concentrations in *R. pachyptila* mixed blood and coelomic fluid as a function of the $\sum H_2S$ concentrations in the aquaria. (B) trophosome sulfur content as a function of $\sum H_2S$ concentrations in *R. pachyptila* mixed blood and coelomic fluid. Open symbols indicate low $\sum H_2S$ aquaria, and filled symbols indicate high $\sum H_2S$ aquaria. Error bars indicate the standard deviations of the data.

to 4.9- and 4.1-fold increases. In contrast, RubisCO transcript abundance did not differ between low and high $\sum H_2S$ treatments.

Stable isotope compositions of lipids and biomass. The $\delta^{13}C$ values of fatty acids and biomass from trophosome samples and "*Ca.* E. persephonae" from freshly collected *R. pachyptila* samples suggest input from both the rCAC and CBB (Table 5). Trends from *Hydrogenovibrio crunogenus* and *Chlorobium tepidum* are consistent with their CO_2 fixation pathways (CBB and rCAC, respectively); relative to biomass, lipids from *H. crunogenus* were ^{13}C depleted, and *C. tepidum* lipids were enriched (Table 5). Lipids from *R. pachyptila* trophosome samples and "*Ca.* Endoriftia persephonae" were also enriched in ^{13}C, but to a lesser extent than those measured for autotrophs relying entirely on the rCAC (Table 5).

DISCUSSION

We hypothesized that "*Ca.* E. persephonae" would predominantly use the rCAC for CO_2 fixation when exposed to low $\sum H_2S$ conditions, since the rCAC requires less

TABLE 1 Rank correlations between internal and external sulfur compounds in *Riftia pachyptila* maintained in high-pressure aquaria

Comparison[b]	r^2	Positive or negative	F	P	n[a]
Blood and CF $\sum H_2S$ vs $\sum H_2S$ supply rate	0.647	+	16.5	0.002	11
Blood and CF $\sum H_2S$ vs $[\sum H_2S]$ in aquarium	0.582	+	26.4	0.000	21
Trophosome sulfur content vs $\sum H_2S$ supply rate	0.303	+	3.91	0.079	11
Trophosome sulfur content vs $[\sum H_2S]$ in aquarium	0.159	+	1.70	0.225	11
Trophosome sulfur content vs blood and CF $[\sum H_2S]$	0.506	+	9.21	0.014	11

[a]No. of *R. pachyptila* individuals.
[b]CF, coelomic fluid.

TABLE 2 Rank correlations between sulfur compounds and CO_2 fixation parameters in *Riftia pachyptila* maintained in high-pressure aquaria

Comparison[b]	r^2	Positive or negative	F	P	n[a]
Trophosome CO_2 fixation rate vs $\sum H_2S$ supply rate	0.113	+	1.15	0.312	11
Trophosome CO_2 fixation rate vs $[\sum H_2S]$ in aquarium	0.044	+	0.41	0.537	11
Trophosome CO_2 fixation rate vs blood and CF $[\sum H_2S]$	0.013	+	0.12	0.739	11
Trophosome CO_2 fixation rate vs trophosome sulfur content	0.001	−	0.01	0.912	11
RubisCO activity vs $\sum H_2S$ supply rate	0.021	+	0.19	0.670	11
RubisCO activity vs $[\sum H_2S]$ in aquarium	<0.001	−	<0.01	0.958	11
RubisCO activity vs blood and CF $[\sum H_2S]$	0.003	−	0.02	0.878	11
RubisCO activity vs trophosome sulfur content	0.007	+	0.07	0.803	11
ACL activity vs $\sum H_2S$ supply rate	0.004	−	0.04	0.853	11
ACL activity vs $[\sum H_2S]$ in aquarium	<0.001	+	<0.01	0.958	11
ACL activity vs blood and CF $[\sum H_2S]$	0.099	−	0.99	0.346	11
ACL activity vs trophosome sulfur content	0.199	−	2.24	0.169	11
$\Delta\delta^{13}C(DIC_{blood\ and\ CF} - DIC_{aquarium})$[c] vs $\sum H_2S$ supply rate	0.024	+	0.22	0.649	11
$\Delta\delta^{13}C(DIC_{blood\ and\ CF} - DIC_{aquarium})$ vs $[\sum H_2S]$ in aquarium	0.028	+	0.41	0.533	11
$\Delta\delta^{13}C(DIC_{blood\ and\ CF} - DIC_{aquarium})$ vs blood and CF $[\sum H_2S]$	0.122	+	1.80	0.203	11
$\Delta\delta^{13}C(DIC_{blood\ and\ CF} - DIC_{aquarium})$ vs trophosome sulfur content	0.079	+	0.77	0.403	11
$\Delta\delta^{13}C(DIC_{trophosome} - DIC_{aquarium})$ vs $[\sum H_2S]$ in aquarium	0.305	+	1.75	0.256	6
$\Delta\delta^{13}C(DIC_{trophosome} - DIC_{aquarium})$ vs blood and CF $[\sum H_2S]$	0.516	−	3.20	0.172	5
$\Delta\delta^{13}C(DIC_{trophosome} - DIC_{blood\ and\ CF})$ vs $[\sum H_2S]$ in aquarium	0.750	−	9.00	0.058	5
$\Delta\delta^{13}C(DIC_{trophosome} - DIC_{blood\ and\ CF})$ vs blood and CF $[\sum H_2S]$	0.800	−	3.56	0.200	4

[a]No. of *R. pachyptila* individuals.
[b]CF, coelomic fluid; ACL, ATP-dependent citrate lyase.
[c]$\Delta\delta^{13}C(DIC_a - DIC_b) = (\Delta\delta^{13}C \text{ of } DIC_a) - (\Delta\delta^{13}C \text{ of } DIC_b)$.

energy to synthesize biomass from CO_2 than the CBB does (24). The results from this study did not provide strong support for this hypothesis. Trophosome CO_2 fixation rates, enzyme activities, and $\Delta\delta^{13}C$ values varied considerably between samples collected from different *R. pachyptila* and did not correlate with $\sum H_2S$ supply to aquaria in which they had been maintained (Table 2 and Fig. 3; see also Tables S1 to S3 in the supplemental material). The abundance of transcripts of the gene encoding RubisCO were similar under low $\sum H_2S$ versus high $\sum H_2S$ conditions (Fig. 4). Transcripts of genes encoding the two subunits of ACL were the only parameters to have a consistent and measurable response to $\sum H_2S$ supply, with their abundance moderately elevated (4.1- to 4.9-fold more abundant) under low $\sum H_2S$ conditions (Fig. 4). Based on these results, which are the first to be collected for *R. pachyptila* samples whose environmental conditions were extensively measured prior to analysis, the environmental $\sum H_2S$ conditions tested here do not result in large changes in the use of the rCAC or the CBB.

In order for this conclusion to be warranted, it is necessary for *R. pachyptila* to have been maintained for sufficient time for the conditions within *R. pachyptila*, where "*Ca.* E. persephonae" is housed, to reflect external conditions. This does appear to have been the case for the *R. pachyptila* samples used for this study, which had been maintained under low or high $\sum H_2S$ conditions for 48 to 72 h. Their internal sulfur stores (blood and coelomic fluid $\sum H_2S$ and trophosome elemental sulfur content) reflected external $\sum H_2S$ concentrations. Low $\sum H_2S$ conditions resulted in lower $\sum H_2S$ concentrations in the blood and coelomic fluid, and *R. pachyptila* with elevated $\sum H_2S$ concentrations in the blood and coelomic fluid had higher trophosome elemental sulfur content (Table 1 and Fig. 2). Since internal sulfur availability reflected external $\sum H_2S$ conditions, it is reasonable to expect that if the rCAC or the CBB were differentially regulated in response to environmental $\sum H_2S$, there should have been a measurable and consistent change in the CO_2 fixation parameters measured here.

Given that ACL transcript levels were elevated under low $\sum H_2S$ conditions, it is puzzling that ACL enzyme activities were not (Fig. 3 and Table 2). It is likely that the ACL activities measured in trophosome samples were a mixture of animal and bacterial ACL activities, since ACL activities were also detected in samples of *R. pachyptila* vestimentum, which do not contain symbionts (see Table S4 in the supplemental material). The host tubeworm, like other animals, may be using ACL for fatty acid biosynthesis (52). The

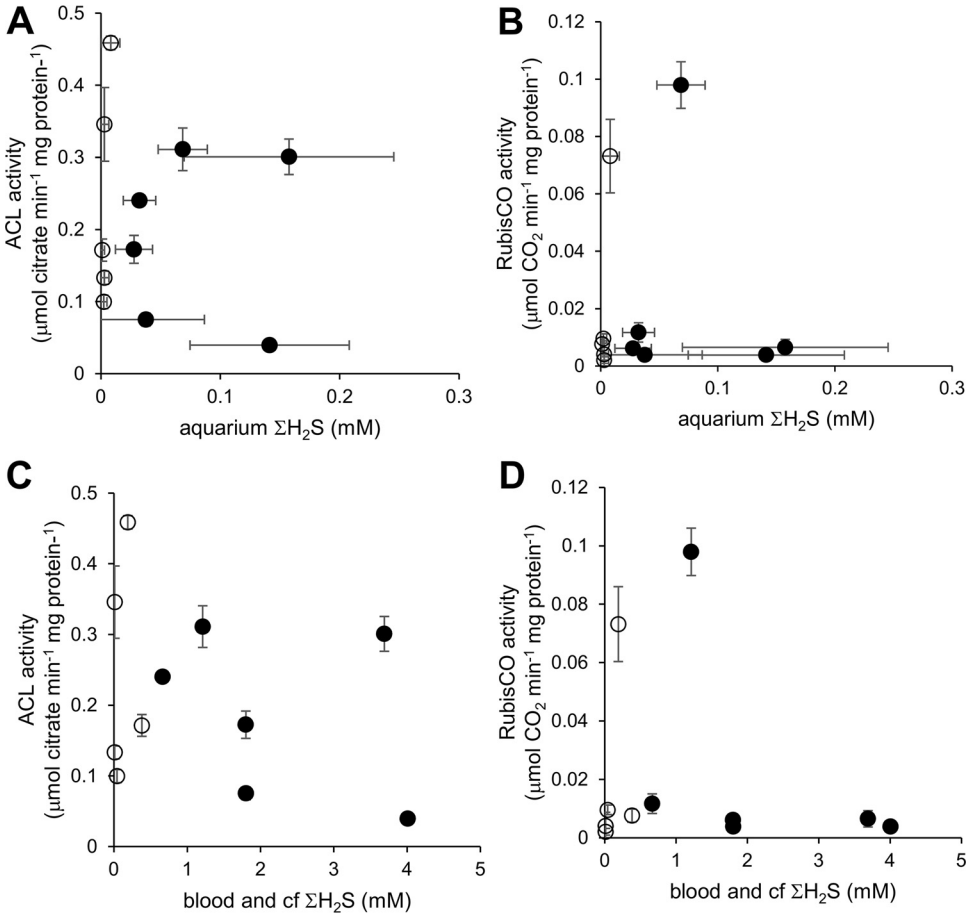

FIG 3 Enzyme activities of trophosome samples from *Riftia pachyptila* maintained in high-pressure flowthrough aquaria. (A) ATP-dependent citrate lyase (ACL activity and (B) RubisCO activity as a function of $\sum H_2S$ concentrations in the aquaria. (C) ACL activity and (D) RubisCO activity as a function of the $\sum H_2S$ concentrations in *R. pachyptila* mixed blood and coelomic fluid. Open symbols indicate low $\sum H_2S$ aquaria, and filled symbols indicate high $\sum H_2S$ aquaria. Error bars indicate the standard deviations of the data.

presence of "animal" ACL activities could obscure differences in levels of "bacterial" ACL in trophosome samples, especially if these differences are small. It is difficult to predict the differences in enzyme activity resulting from 4.1- to 4.9-fold differences in bacterial ACL transcript levels. Differences of a similar magnitude (~5-fold higher) in transcript abundance for the gene encoding "*Ca.* E. persephonae" RubisCO were correlated with a

TABLE 3 Rank correlations between oxygen and CO_2 fixation parameters in *Riftia pachyptila* maintained in high-pressure aquaria

Comparison[b]	r^2	Positive or negative	F	P	n[a]
Trophosome CO_2 fixation rate vs O_2 supply rate	0.250	+	3.00	0.118	11
Trophosome CO_2 fixation rate vs $[O_2]$ in aquarium	0.056	+	0.53	0.484	11
RubisCO activity vs O_2 supply rate	0.126	+	1.29	0.284	11
RubisCO activity vs $[O_2]$ in aquarium	0.040	−	0.38	0.555	11
ACL activity vs O_2 supply rate	0.010	+	0.09	0.770	11
ACL activity vs $[O_2]$ in aquarium	<0.001	−	<0.01	0.979	11
$\Delta\delta^{13}C(DIC_{blood\ and\ CF} - DIC_{aquarium})$[c] vs O_2 supply rate	0.088	−	0.87	0.377	11
$\Delta\delta^{13}C(DIC_{blood\ and\ CF} - DIC_{aquarium})$ vs $[O_2]$ in aquarium	0.260	−	4.92	0.044	16
$\Delta\delta^{13}C(DIC_{trophosome} - DIC_{aquarium})$ vs $[O_2]$ in aquarium	0.857	+	24.00	0.008	6
$\Delta\delta^{13}C(DIC_{trophosome} - DIC_{blood\ and\ CF})$ vs $[O_2]$ in aquarium	0.900	+	27.00	0.014	5

[a]No. of *R. pachyptila* individuals.
[b]ACL, ATP-dependent citrate lyase.
[c]$\Delta\delta^{13}C(DIC_a - DIC_b) = (\Delta\delta^{13}C \text{ of } DIC_a) - (\Delta\delta^{13}C \text{ of } DIC_b)$.

TABLE 4 Rank correlations among CO_2 fixation parameters in *Riftia pachyptila* maintained in high-pressure aquaria

Comparison[b]	r^2	Positive or negative	F	P	n[a]
RubisCO activity vs trophosome CO_2 fixation rate	0.001	−	<0.01	0.937	11
ACL activity vs trophosome CO_2 fixation rate	0.036	−	0.34	0.574	11
ACL activity vs RubisCO activity	0.349	+	4.83	0.056	11
$\Delta\delta^{13}C(DIC_{blood\ and\ CF} - DIC_{vessel})$[c] vs RubisCO activity	0.065	+	0.63	0.449	11
$\Delta\delta^{13}C(DIC_{blood\ and\ CF} - DIC_{vessel})$ vs ACL activity	0.030	+	0.28	0.611	11
$\Delta\delta^{13}C(DIC_{blood\ and\ CF} - DIC_{vessel})$ vs trophosome CO_2 fixation rate	0.143	−	1.50	0.252	11

[a]No. of *R. pachyptila* individuals.
[b]ACL, ATP-dependent citrate lyase.
[c]$\Delta\delta^{13}C(DIC_a - DIC_b) = (\Delta\delta^{13}C \text{ of } DIC_a) - (\Delta\delta^{13}C \text{ of } DIC_b)$.

1.8-fold higher abundance of RubisCO protein (32). This raises the possibility that the differences in ACL transcript abundance measured in this study also resulted in small differences in symbiont ACL activity, which could have been obscured by the presence of "animal" ACL activities in trophosome samples.

What is clear is that further exploration is needed to decipher whether environmental cues could influence the proportion of CO_2 fixed by the rCAC and the CBB in this symbiosis. One possibility is that it may take longer than 48 to 72 h for the CO_2-fixing pathway expressed by "*Ca.* E. persephonae" to respond to conditions external to the host. If logistically possible, it would be good to determine whether longer exposures to different environmental conditions would elicit the anticipated changes. Alternatively, it is possible that exposure to a larger span in environmental $\sum H_2S$ concentrations could make up- or down-regulation more obvious. However, the $\sum H_2S$ concentrations chosen for this study reflect those present *in situ*, making interpreting the results from a broader range problematic. Another possible approach would be to explore the influence of oxygen concentrations,

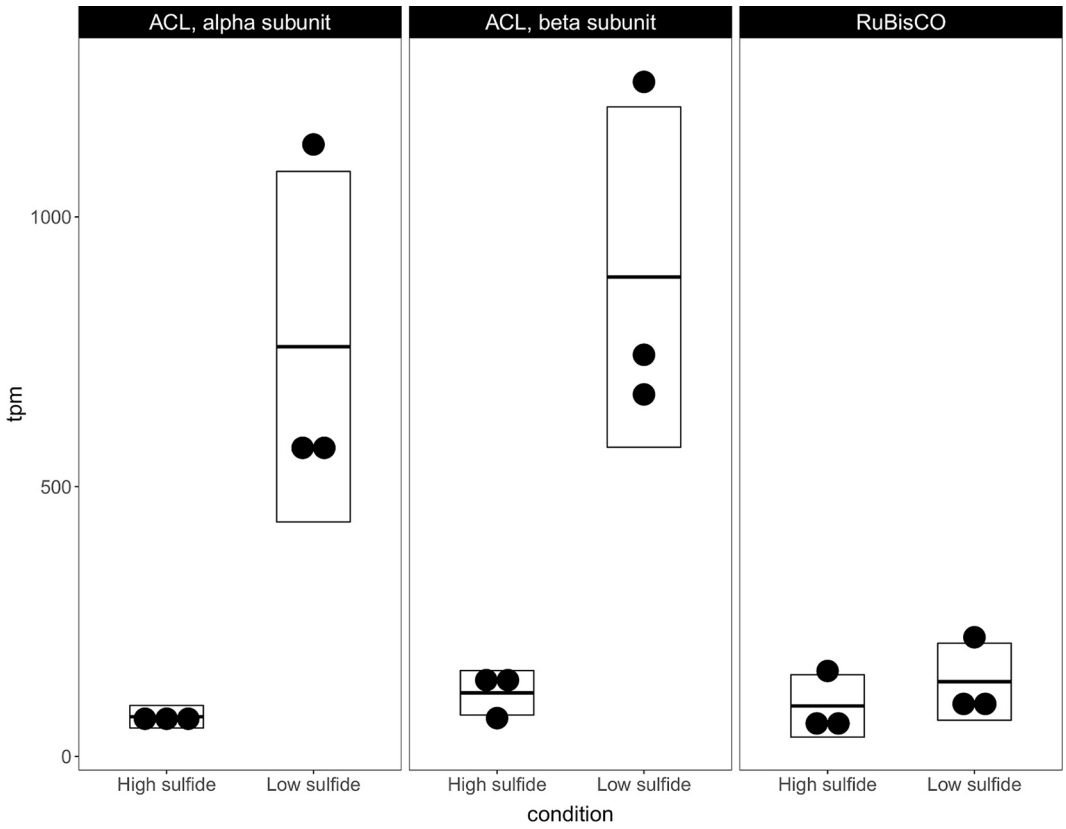

FIG 4 Transcripts per million (tpm) from genes encoding primary enzymes from the rCAC (ACL alpha and beta subunits) and the CBB (RubisCO), from *Riftia pachyptila* individuals maintained in high-pressure aquaria under high or low $\sum H_2S$ conditions. Each black circle represents transcripts from a different *R. pachyptila* specimen (3 per treatment). Boxes represent the mean and two standard deviations from the mean.

TABLE 5 Stable isotope composition of autotrophic microorganisms and bulk biomass and lipids from trophosome and symbiont samples from freshly collected *Riftia pachyptila*

Sample	Autotrophic pathway[a]	Biomass $\delta^{13}C$ (‰)[b]	16:0 $\delta^{13}C$[c] (‰)	18:0 $\delta^{13}C$[c] (‰)	$\varepsilon_{biomass/16:0}$[d] (‰)	$\varepsilon_{biomass/18:0}$ (‰)
Synechocystis UTEX 2470	CBB				7.6[e]	
Nitrosomonas europaea	CBB				6.9[e]	
Allochromatium vinosum	CBB				4.8[e]	
Hydrogenovibrio crunogenus	CBB	−39.9	−44.3 ± 0.9	−46.9 ± 0.6	4.4	7
"*Ca*. Endoriftia persephonae"[f]		−13.7	−12.2 ± 0.3	−14.2 ± 1.9	−1.5	0.5
R. pachyptila 1 trophosome		−13.5	−11.9 ± 0.3	−7.1 ± 1.6	−1.6	−6.4
R. pachyptila 2 trophosome		−9.8	−7.5 ± 0.2	−5.1 ± 1.4	−2.3	−4.7
"*Ca*. Endoriftia persephonae" from *R. pachyptila* 2 trophosome[f]		−9.9	−6.8 ± 0.4	−6.6 ± 0.9	−3.1	−3.3
Magnetococcus sp.	rCAC				−3.6[e]	
R. pachyptila trophosome		−13.7	−8.8 ± 0.1	−9.0 ± 2.1	−4.9	−4.7
"*Ca*. Endoriftia persephonae" from *R. pachyptila* 1 trophosome[f]		−13.7	−8.6 ± 0.4	−7.1 ± 1.1	−5.1	−6.6
Chlorobium tepidum	rCAC	−20.4	−11.3 ± 0.4	ND	−9.1	
Chlorobium limnicola	rCAC				−16[e]	

[a]CBB, Calvin-Benson-Bassham cycle; rCAC, reductive citric acid cycle.
[b]Standard deviation of biomass $\delta^{13}C$ values is approximately 0.2‰.
[c]16:0 and 18:0 are palmitic and stearic acids, respectively, and are ± standard deviation.
[d]$\varepsilon_{biomass/16:0}$ = biomass $\delta^{13}C$ − 16:0 $\delta^{13}C$; $\varepsilon_{biomass/18:0}$ = biomass $\delta^{13}C$ − 18:0 $\delta^{13}C$.
[e]Values are from references 61 and 75−77.
[f]"*Ca*. Endoriftia persephonae" was enriched from trophosome samples by centrifugation through Percoll.

especially given that the rCAC in many organisms is more sensitive to oxygen than the CBB (22). Care was taken here to prevent correlations between $\sum H_2S$ concentrations and oxygen concentrations and to prevent oxygen concentrations from getting very low (Table 6 and Fig. 1C). It would be interesting to determine whether the relative inputs from the rCAC and the CBB responded to oxygen concentrations under conditions where the $\sum H_2S$ was maintained at particular target values. Genes encoding seven oxoacid:ferredoxin oxidoreductases are present in the incomplete "*Ca.* E. persephonae" genome. Among these seven proteins, pyruvate synthase (EC 1.2.7.1) and 2-oxoglutarate synthase (EC 1.2.7.3) are needed for the rCAC to operate. In *Hydrogenobacter thermophilus*, a more oxygen-tolerant version of 2-oxoglutarate synthase facilitates growth under low-oxygen conditions (53). The presence of multiple isoforms of either or both of these enzymes in "*Ca.* E. persephonae" may be an adaptation for maintaining rCAC function when oxygen concentrations vary.

It is also clear that both the rCAC and CBB are active in "*Ca.* E. persephonae." Differences in $\delta^{13}C$ values between fatty acids and biomass ($\varepsilon_{biomass/16:0}$ and $\varepsilon_{biomass/18:0}$; Table 5) fall between the ranges measured for organisms using either the rCAC or the CBB. It is possible that both pathways are constitutively expressed, providing "*Ca.* E. persephonae" with the advantage of being able to provide intermediates from either cycle to its host in the presence of variable concentrations of environmental $\sum H_2S$ and oxygen. This could be an advantage because the rCAC and the CBB rely on different cellular electron carriers (ferredoxin-rCAC versus NADH/NADPH-CBB and -rCAC); the simultaneous activity of both pathways could help to maintain redox balance within the trophosome. A similar role for redox balance maintenance has been suggested for "*Ca.* E. persephonae" hydrogenase (54).

"*Ca.* E. persephonae" was the first bacterium discovered to have the potential to express both the CBB and the rCAC (15). Since then, the genetic potential to use both pathways has been observed in "*Ca.* Thiomargarita nelsonii" and *Thioflavicoccus mobilis*, free-living members of *Gammaproteobacteria*, as well as in the symbionts from multiple vestimentiferans (19–21). It has also been observed that citrate synthase can operate in a citrate cleaving direction, and the CAC can operate in a reductive, CO_2-fixing direction to facilitate autotrophic growth in organisms lacking ACL genes (55–57). All of these observations suggest that dual activities of these two pathways within a single organism may be more prevalent than once thought. This in turn highlights the importance of uncovering the advantages that operating both the CBB and the rCAC might offer to these organisms, whether differentially regulated or not.

TABLE 6 Rank correlations between environmental parameters in high-pressure aquaria

Comparison	r^2	Positive or negative	F	P	n^a
$[\sum H_2S]$ in aquarium vs $\sum H_2S$ supply rate	0.877	+	64.00	0.000	11
$[O_2]$ in aquarium vs O_2 supply rate	0.308	+	3.997	0.077	11
O_2 supply rate vs $\sum H_2S$ supply rate	0.008	+	0.075	0.794	11
$[O_2]$ vs $[\sum H_2S]$ in aquarium	0.109	−	1.707	0.212	16

[a]No. of aquaria.

MATERIALS AND METHODS

***R. pachyptila* collection and maintenance.** *R. pachyptila* individuals were collected from hydrothermal vent fields at the 9°N Integrated Study Site in the East Pacific (9°50′N, 104°18′W, 2,500-m depth) using the human-occupied vehicle (HOV) *Alvin* during November 2014 (*Alvin* cruise AT-26) and October 2016 (*Alvin* cruise AT-37). Collections of *R. pachyptila* took place at the end of the *Alvin* dive. Individuals small enough to maintain in high-pressure aquaria (3 to 18 g) were placed in a thermally insulated Biobox during the 1-h transit to the surface, where they were either sampled immediately (see details below) or individually incubated in high-pressure aquaria under *in situ* conditions (250 atm; DIC = 2.7 to 4.1 mM; O_2 = 0.02 to 0.26 mM; pH = 5.9 to 6.7; 15°C [14]). Viability was monitored for 12 h via observation ports to verify minimal damage to the worms during collection.

Subsequently, $\sum H_2S$ was supplied to the aquaria at either of two rates in order to generate concentrations inside the aquaria that bracket those present among *R. pachyptila in situ*, namely, low $\sum H_2S$ supply (28 to 40 μmol · h^{-1}, resulting in <0.001 to 0.008 mM $\sum H_2S$ in the aquaria) or high $\sum H_2S$ supply (180 to 275 μmol · h^{-1}, resulting in 0.032 to 0.141 mM in the aquaria). Rates of $\sum H_2S$ supply correlated strongly with $\sum H_2S$ concentrations in the aquaria, but not with oxygen supply or concentration (Fig. 1 and Table 6). *R. pachyptila* incubated under these conditions had previously been shown to have very different metabolic rates, with worms incubated under $\sum H_2S$ conditions having considerably higher rates of DIC uptake, suggesting a potential shift in metabolic mode (14). Worms were maintained under these conditions for 48 to 72 h, with DIC, $\sum H_2S$, and oxygen concentrations in the aquaria monitored via gas chromatography (58) and pH via an AR15 pH meter (Accumet) equipped with a calomel-referenced pH electrode (Fisher Scientific, Pittsburg, PA) calibrated with National Bureau of Standards (NBS) standards (pH 4.0, 7.0, and 10.0).

Worms were removed for tissue analyses and trophosome preparations by depressurizing the aquaria rapidly (~5 min); they were then immediately dissected in a cold room (10°C). Mixed samples of vascular and coelomic fluid were drawn into gastight syringes and stored refrigerated, and dissolved gases were quantified within 6 h. Trophosome and vestimentum samples for enzyme assays, sulfur, and $\delta^{13}C$ analyses of organic carbon were immediately freeze-clamped and stored at −80°C. Trophosome samples were also taken for immediate ^{14}C assays for autotrophic potential and were prepared as described below. Mixed samples of vascular blood and coelomic fluid, as well as trophosome, were also removed for $\delta^{13}C$ analyses of DIC, as described below.

Impact of $\sum H_2S$ supply on *R. pachyptila* tissues. $\sum H_2S$ concentrations in vascular and coelomic fluid were quantified with a gas chromatograph front-ended with an extractor that facilitated stripping dissolved gases from these fluids when acidified, and by introducing the gases into a two-column system to resolve them for quantification with a thermal conductivity detector (58). The elemental sulfur content of trophosome samples was determined at the USF Stable Isotope Lab with an ECS4010 elemental analyzer (Costech, Valencia, CA), using the Mass 66 collector on a Delta V Advantage isotope ratio mass spectrometer (Thermo Fisher Scientific, Waltham, MA) as the detector, calibrated with organic standards ranging from 0.09 to 5.59% sulfur (59).

Impact of $\sum H_2S$ supply on symbiont CO_2 fixation parameters. To determine whether $\sum H_2S$ availability in aquaria influenced the autotrophic potential of the bacterial endosymbionts, trophosome samples were taken from *R. pachyptila* individuals incubated under high or low $\sum H_2S$ conditions. These samples were homogenized, and their rates of CO_2 fixation were measured radiometrically as in Scott et al. (50), with DIC raised to 10 mM to ensure that CO_2 fixation was CO_2 saturated (60). ^{14}C-DIC was added (50), and incubations were conducted at 18°C in 5-ml stainless steel high-pressure syringes, maintained at 250 atm with a neMESYS high pressure syringe system (Cetoni GMBH, Korbussen, Germany). Syringe contents were agitated with stir bars and micro stir plates. Samples were removed at 5-min intervals for a 30-min time course and were added to 100 μl 1.2 N HCl in a scintillation vial, vortexed, and sparged with air for 2 h to remove residual CO_2. Samples were treated to minimize scintillation quenching caused by trophosome. They were bleached for 20 min with 20 μl H_2O_2 and 200 μl ScintiGest (Fisher Scientific). Scintillation fluid (3 ml of ScintiVerse BD scintillation cocktail; Fisher Scientific) was added to the vials. After 12 h, radioactivity was measured on a scintillation counter.

Trophosome and vestimentum extracts for enzyme assays were prepared from samples stored at −80°C. Samples (0.1 to 0.5 g) were homogenized in 3 ml ice-cold sonication buffer [30 mM $MgCl_2$, 10 mM $NaHCO_3$, 1 mM Na_2EDTA, 2.5 mM dithioerythritol (DTE), and 100 mM sodium 4-(2-hydroxyethyl)-1-piperazineethanesulfonic acid (NaHEPES) (pH 7.5)], supplemented with 0.5 g acid-washed glass beads (<160 μm; Sigma, St. Louis, MO), and sonicated on ice (3 × 15 s, determined to maximize enzyme activity release; data not shown) using a sonic dismembrator (Fisher Scientific, Pittsburgh, PA). Between

sonications, samples were bubbled gently for 1 min with argon while on ice. Sonicate was centrifuged (5 min, 4°C, 10,000 × *g*). High rates of NADH oxidation in ACL assays without added substrate were diminished by desalting the extracts; therefore, for all assays, supernatant was desalted into sonication buffer with PD-10 desalting columns (GE Healthcare, Buckinghamshire, UK).

ACL was assayed spectrophotometrically by tracking oxaloacetate synthesis from citrate, combining previous methods (61, 62), conducted at 20°C. Although ACL activity has been found to be robust under aerobic conditions when reducing agents are present (e.g., DTE [63, 64]), assays were conducted under anaerobic conditions as a precaution. Assay buffer (30 mM $MgCl_2$, 5 mM DTE, and 30 mM Na-HEPES [pH 8]) was sparged with argon, and 1-ml portions were sealed in gastight cuvettes (Pyrex). Adenosine 5′-triphosphate disodium salt (1.5 mM), coenzyme A-free acid trihydrate (0.1 mM), β-NAD, disodium salt, hydrate (NADH, 0.1 mM), and malate dehydrogenase (200 U, from porcine heart, EC 1.1.1.37; MP Biomedicals, Solon, OH) were added to the cuvette. Final concentrations are shown in parentheses. Desalted homogenate was added, and sodium citrate was injected to begin the reaction (0.1 mM final concentration). Activity was determined spectrophotometrically while sealed under an argon headspace. Oxaloacetate produced by ACL was reduced to malate via malate dehydrogenase, and NADH oxidation by this enzyme was monitored via A_{340} measurements taken every 30 s for 2.5 min (ε_{340} = 6.2 $mM^{-1} \cdot cm^{-1}$). ACL activities were calculated by subtracting the rates measured in the absence of added citrate from those in which this substrate was added. ATP-independent citrate lyase activity [e.g., via citrate (pro-3S)-lyase, EC 4.1.3.6] was not anticipated, as this enzyme is not encoded in the symbiont genome. However, it should be noted that if any ATP-independent citrate lyase activity is present, it was included in values determined here.

RubisCO was assayed radiometrically, with a modified protocol based on Schwedock et al. (65), conducted at 20°C. Assay buffer (10 mM $NaHCO_3$, 30 mM $MgCl_2$, 2.5 mM DTE, and 100 mM NaHEPES [pH 7.5]) was bubbled with argon, and 430-μl portions were sealed in glass vials with argon headspace. Trophosome extract (50 μl) and ribulose 1,5-bisphosphate sodium salt hydrate (10 μl, 0.1 mM final concentration) were added, and 10 μl $NaH^{14}CO_3$ solution was injected to begin the reaction (50 mCi/mmol; MP Biomedicals, Santa Ana, CA). Samples (100 μl) were removed at 20-s intervals over a 2-min time course and treated as described above for assays of symbiont autotrophic potential.

For both ACL and RubisCO, pilot assays were conducted to determine temperatures and pH values where activity was high, verify that activity was stimulated by substrate, and to determine whether measured activity was proportional to the amount of extract added (see Fig. S1 in the supplemental materials). Protein concentrations in the assays were measured using an RC DC Protein assay kit (Bio-Rad).

Natural-abundance $\delta^{13}C$ values were determined for DIC in aquarium water, samples of mixed vascular and coelomic fluid, and liquified trophosome (the trophosome disruption protocol is described below). For DIC samples, 12-ml exetainers were loaded with 1 ml 10 mM $CuSO_4$ in 43% phosphoric acid, sealed, and flushed with helium. Aquarium water and body fluids (0.1 to 0.5 ml) were injected into these vials, shaken to acidify them, and stored for <2 months; samples stored this way were stable (data not shown). Samples were analyzed at the USF Stable Isotope Lab with a Delta V Advantage isotope ratio mass spectrometer (Thermo Fisher Scientific).

Prior to injection into exetainers, trophosome samples were liquefied as follows: two glass Luer-Lok gastight syringes were prepared for each sample. One contained 2 ml deionized, distilled water bubbled with argon and verified, via gas chromatography, to be DIC free. Trophosome (0.5 to 1 g) was sealed into the other syringe with zero headspace. Both syringes were coupled to the ends of a 22-gauge emulsifying needle, and distilled water was injected into the syringe containing the trophosome sample. Trophosome and distilled water were passed through the needle 2 or 3 times, and a 0.1- to 0.5-ml portion of this fluid was injected into an exetainer prepared as described above. To verify that liquification did not affect trophosome DIC $\delta^{13}C$ values, 7.5 mM DIC was dissolved in saline with ionic composition similar to that of *R. pachyptila* vascular blood (66), and this saline was treated using the same protocol as for trophosome samples. The stable isotope composition of the DIC in the saline before treatment (-1.4 ± 0.1‰; $n = 2$) and after treatment (-1.5 ± 0.0‰; $n = 3$) were similar.

R. pachyptila trophosome and vestimentum samples were prepared for measurement of organic carbon $\delta^{13}C$ values by fuming 100-mg samples overnight with 12 N HCl and drying them at 60°C for 48 h. $\delta^{13}C$ values were measured by continuous flow elemental analyzer isotope ratio mass spectrometry (CF-EA-IRMS) at the University of South Florida College of Marine Science Stable Isotope Biogeochemistry Laboratory using commonly accepted procedures (67). Isotope compositions were measured on a Thermo Finnigan Delta+XL isotope ration mass spectrometer (Thermo Finnigan). Secondary reference materials (NIST 8574 $\delta^{13}C = +37.63 \pm 0.10$ ‰; NIST 8573 $\delta^{13}C = -26.39 \pm 0.09$‰) were used to normalize raw measurements to the VPDB ($\delta^{13}C$) scale (68–70). Measurement uncertainties, expressed as ± 1 standard deviation of $n = 5$ measurements of a laboratory reference material (NIST 1570a $\delta^{13}C = -27.17 \pm 0.19$‰) were ± 0.23‰.

Impact of $\sum H_2S$ supply rate on transcription of genes encoding CBB and rCAC enzymes. Symbiont-containing trophosome samples were excised from *R. pachyptila* individuals maintained under high and low $\sum H_2S$ conditions. Samples were immediately homogenized and stored in TRIzol reagent at −80°C. Total RNA was extracted and rRNA removed, and mRNA was sequenced and analyzed as described previously (54). Transcripts for ACL subunit alpha, ACL subunit beta, and RuBisCO (GenBank accession numbers WP_005962054.1, EGW53537.1, and WP_005960001.1, respectively) were calculated using *kallisto* and *sleuth*, as described previously (54).

Stable isotope compositions of lipids and biomass from freshly collected *R. pachyptila* individuals. Samples from *R. pachyptila* individuals freshly recovered from the vents were used to determine $\delta^{13}C$ values for lipids extracted from trophosome, vestimentum, and "*Ca.* E. persephonae" enriched from fresh

trophosome samples via centrifugation through Percoll (60). For comparison, lipids were also extracted from *Hydrogenovibrio crunogenus* (CBB) and *Chlorobium tepidum* (rCAC). Both organisms were cultivated autotrophically (58, 71), and cell pellets were stored at −80°C until use. *C. tepidum* pellets were kindly provided by Thomas Hanson (University of Delaware), and *H. crunogenus* XCL-2 (72) was originally provided by Douglas Nelson (UC Davis). Lipids were extracted and derivatized as described previously (73). At the University of South Florida College of Marine Science Stable Isotope Biogeochemistry Laboratory, samples were evaporated under ultrahigh-purity N_2 streams to dryness and rehydrated to 1 ml in hexane (GC-Resolve; Fisher Scientific). Aliquots (100 μl) were split into autosampler vials for injection. Samples were prescreened for target compound presence and concentration on a Varian 3800-GC/310-MS system (scanning 50 to 500 atomic mass units [AMU], HP DB-Wax column [30 m × 0.25 mm × 0.25 μm], initial temperature of 50°C, 3-min hold; 30°C/min to 120°C; 8°C/min to 355°C, 5.0-min hold). Splitless injections (1 to 4 μl depending on relative concentration of target compounds) were chromatographed through an Agilent 6890A gas chromatograph (GC) using the using the same column and program described above. Chromatographed compounds were transmitted through a modified GC-Combustion-III oxidation reactor (Thermo Fisher) and open-split interface into a Delta+XL IRMS analyzer for measurement. Raw measurements were normalized to the VPDB scale using an esterified known octadecanoic acid laboratory reference material ($\delta\ ^{13}C = -28.73 \pm 0.09‰$).

Statistics. Rank regressions were used to determine whether physiological parameters and enzyme activities from *R. pachyptila* individuals correlated with $\sum H_2S$ or oxygen supply, or correlated with each other. Values were ranked from smallest to largest and regressed against each other. Rank regressions were used, as the nature of the relationships between the parameters was not known and rank regressions are robust to nonlinearity in the relationships (74).

To compare transcript levels from *R. pachyptila* individuals incubated under low or high $\sum H_2S$ supply rates, a Wald test was done in R using the *sleuth* package, with the function "(sleuth_prep(. . . . ., transformation_function=function(x) $\log_2$(x +0.5)))," which provides β values, which are biased estimates of $\log_2$ fold change.

Data availability. Transcriptome data have been deposited under accession number PRJNA736714 in the NCBI BioProject database.

SUPPLEMENTAL MATERIAL

Supplemental material is available online only.

SUPPLEMENTAL FILE 1, PDF file, 0.1 MB.

ACKNOWLEDGMENTS

We are grateful to Thomas Hanson for providing *Chlorobium tepidum* biomass for this study and to anonymous reviewers for their helpful comments.

We are also grateful for support from the National Science foundation (grants NSF-IOS-1257532 and NSF-MCB-1952676 to K.M.S. and NSF-IOS-1257755 to P.R.G.).

REFERENCES

1. Bright M, Lallier FH. 2010. The biology of vestimentiferan tubeworms, p 213–266. *In* Gibson RN, Atkinson JA, Gordon JDM (ed), Oceanography and marine biology: an annual review, vol 48. CRC Press, Boca Raton, FL.
2. Corliss JB, Dymond J, Gordon LI, Edmond JM, von Herzen RP, Ballard RD, Green K, Williams D, Bainbridge A, Crane K, van Andel TH. 1979. Submarine thermal springs on the Galapagos Rift. Science 203:1073–1083. https://doi.org/10.1126/science.203.4385.1073.
3. Cordes EE, Bergquist DC, Fisher CR. 2009. Macro-ecology of Gulf of Mexico cold seeps. Annu Rev Mar Sci 1:143–168. https://doi.org/10.1146/annurev.marine.010908.163912.
4. Bergquist DC, Eckner JT, Urcuyo IA, Cordes EE, Hourdez S, Macko SA, Fisher CR. 2007. Using stable isotopes and quantitative community characteristics to determine a local hydrothermal vent food web. Mar Ecol Prog Ser 330:49–65. https://doi.org/10.3354/meps330049.
5. Govenar B, Le Bris N, Gollner S, Glanville J, Aperghis AB, Hourdez S, Fisher CR. 2005. Epifaunal community structure associated with *Riftia pachyptila* aggregations in chemically different hydrothermal vent habitats. Mar Ecol Prog Ser 305:67–77. https://doi.org/10.3354/meps305067.
6. Cavanaugh CM, Gardiner SL, Jones ML, Jannasch HW, Waterbury JB. 1981. Prokaryotic cells in the hydrothermal vent tube worm *Riftia pachyptila* Jones: possible chemoautotrophic symbionts. Science 213:340–342. https://doi.org/10.1126/science.213.4505.340.
7. Felbeck H. 1985. CO_2 fixation in the hydrothermal vent tube worm *Riftia pachyptila* (Jones). Physiol Zool 58:272–281. https://doi.org/10.1086/physzool.58.3.30155998.
8. Childress JJ, Fisher CR, Favuzzi JA, Kochevar RE, Sanders NK, Alayse AM. 1991. Sulfide-driven autotrophic balance in the bacterial symbiont-containing hydrothermal vent tubeworm, *Riftia pachyptila* Jones. Biol Bull 180:135–153. https://doi.org/10.2307/1542437.
9. Bright M, Keckeis H, Fisher CR. 2000. An autoradiographic examination of carbon fixation, transfer and utilization in the *Riftia pachyptila* symbiosis. Mar Biol 136:621–632. https://doi.org/10.1007/s002270050722.
10. Jones ML. 1981. *Riftia pachyptila* Jones: observations on the vestimentiferan worm from the Galapagos Rift. Science 213:333–336. https://doi.org/10.1126/science.213.4505.333.
11. Arp AJ, Childress JJ, Fisher CR. 1985. Blood gas transport in *Riftia pachyptila*. Biol Soc Wash Bull 6:289–300.
12. Flores JF, Fisher CR, Carney SL, Green BN, Freytag JK, Schaeffer SW, Royer J. 2005. Sulfide binding is mediated by zinc ions discovered in the crystal structure of a hydrothermal vent tubeworm hemoglobin. Proc Natl Acad Sci U S A 102:2713–2718. https://doi.org/10.1073/pnas.0407455102.
13. Fisher CR, Childress JJ, Minnich E. 1989. Autotrophic carbon fixation by the chemoautotrophic symbionts of *Riftia pachyptila*. Biol Bull 177:372–385. https://doi.org/10.2307/1541597.
14. Girguis PR, Childress JJ. 2006. Metabolite uptake, stoichiometry and chemoautotrophic function of the hydrothermal vent tubeworm *Riftia pachyptila*: responses to environmental variations in substrate concentrations and temperature. J Exp Biol 209:3516–3528. https://doi.org/10.1242/jeb.02404.
15. Markert S, Arndt C, Felbeck H, Becher D, Sievert SM, Hügler M, Albrecht D, Robidart J, Bench S, Feldman RA, Hecker M, Schweder T. 2007. Physiological proteomics of the uncultured endosymbiont of *Riftia pachyptila*. Science 315:247–250. https://doi.org/10.1126/science.1132913.
16. Markert S, Gardebrecht A, Felbeck H, Sievert SM, Klose J, Becher D, Albrecht D, Thurmer A, Daniel R, Kleiner M, Hecker M, Schweder T. 2011.

Status quo in physiological proteomics of the uncultured *Riftia pachyptila* endosymbiont. Proteomics 11:3106–3117. https://doi.org/10.1002/pmic.201100059.
17. Robidart JC, Roque A, Song P, Girguis PR. 2011. Linking hydrothermal geochemistry to organismal physiology: physiological versatility in *Riftia pachyptila* from sedimented and basalt-hosted vents. PLoS One 6:e21692. https://doi.org/10.1371/journal.pone.0021692.
18. Robidart JC, Bench SR, Feldman RA, Novoradovsky A, Podell SB, Gaasterland T, Allen EE, Felbeck H. 2008. Metabolic versatility of the *Riftia pachyptila* endosymbiont revealed through metagenomics. Environ Microbiol 10:727–737. https://doi.org/10.1111/j.1462-2920.2007.01496.x.
19. Thiel V, Hugler M, Blumel M, Baumann HI, Gartner A, Schmaljohann R, Strauss H, Garbe-Schonberg D, Petersen S, Cowart DA, Fisher CR, Imhoff JF. 2012. Widespread occurrence of two carbon fixation pathways in tubeworm endosymbionts: lessons from hydrothermal vent associated tubeworms from the Mediterranean Sea. Front Microbiol 3:423. https://doi.org/10.3389/fmicb.2012.00423.
20. Winkel M, Salman-Carvalho V, Woyke T, Richter M, Schulz-Vogt HN, Flood BE, Bailey JV, Mußmann M. 2016. Single-cell sequencing of *Thiomargarita* reveals genomic flexibility for adaptation to dynamic redox conditions. Front Microbiol 7:964. https://doi.org/10.3389/fmicb.2016.00964.
21. Rubin-Blum M, Dubilier N, Kleiner M. 2019. Genetic evidence for two carbon fixation pathways (the Calvin-Benson-Bassham cycle and the reverse tricarboxylic acid cycle) in symbiotic and free-living bacteria. mSphere 4:e00394-18. https://doi.org/10.1128/mSphere.00394-18.
22. Berg I. 2011. Ecological aspects of the distribution of different autotrophic CO_2 fixation pathways. Appl Environ Microbiol 77:1925–1936. https://doi.org/10.1128/AEM.02473-10.
23. Lücker S, Wagner M, Maixner F, Pelletier E, Koch H, Vacherie B, Rattei T, Damsté JSS, Spieck E, Le Paslier D, Daims H. 2010. A *Nitrospira* metagenome illuminates the physiology and evolution of globally important nitrite-oxidizing bacteria. Proc Natl Acad Sci U S A 107:13479–13484. https://doi.org/10.1073/pnas.1003860107.
24. Mangiapia M, Scott K. 2016. From CO_2 to cell: energetic expense of creating biomass using the Calvin-Benson-Bassham and reductive citric acid cycles based on genome data. FEMS Microbiol Lett 363.
25. Le Bris N, Govenar B, Le Gall C, Fisher CR. 2006. Variability of physicochemical conditions in 9°50 ′N EPR diffuse flow vent habitats. Mar Chem 98:167–182. https://doi.org/10.1016/j.marchem.2005.08.008.
26. Johnson KS, Childress JJ, Hessler RR, Sakamoto-Arnold CM, Beehler CL. 1988. Chemical and biological interactions in the Rose Garden hydrothermal vent field, Galapagos spreading center. Deep Sea Res 35:1723–1744. https://doi.org/10.1016/0198-0149(88)90046-5.
27. Goffredi SK, Childress JJ, Desaulniers NT, Lee RW, Lallier FH, Hammond D. 1997. Inorganic carbon acquisition by the hydrothermal vent tubeworm *Riftia pachyptila* depends upon high external pCO_2 and upon proton-equivalent ion transport by the worm. J Exp Biol 200:883–896. https://doi.org/10.1242/jeb.200.5.883.
28. Arp AJ, Childress JJ, Fisher CRJ. 1984. Metabolic and blood gas transport characteristics of the hydrothermal vent bivalve *Calyptogena magnifica*. Physiol Zool 57:648–662. https://doi.org/10.1086/physzool.57.6.30155991.
29. Pflugfelder B, Fisher CR, Bright M. 2005. The color of the trophosome: elemental sulfur distribution in the endosymbionts of *Riftia pachyptila* (Vestimentifera; Siboglinidae). Mar Biol 146:895–901. https://doi.org/10.1007/s00227-004-1500-x.
30. Fisher CR, Childress JJ, Arp AJ, Brooks JM, Distel D, Favuzzi JA, Macko SA, Newton A, Powell MA, Somero GN, Soto T. 1988. Physiology, morphology, and biochemical composition of *Riftia pachyptila* at Rose Garden in 1985. Deep Sea Res 35:1745–1758. https://doi.org/10.1016/0198-0149(88)90047-7.
31. Hinzke T, Kleiner M, Breusing C, Felbeck H, Häsler R, Sievert SM, Schlüter R, Rosenstiel P, Reusch TBH, Schweder T, Markert S. 2019. Host-microbe interactions in the chemosynthetic *Riftia pachyptila* symbiosis. mBio 10:e02243-19. https://doi.org/10.1128/mBio.02243-19.
32. Hinzke T, Kleiner M, Meister M, Schlüter R, Hentschker C, Pané-Farré J, Hildebrandt P, Felbeck H, Sievert SM, Bonn F, Völker U, Becher D, Schweder T, Markert S. 2021. Bacterial symbiont subpopulations have different roles in a deep-sea symbiosis. Elife 10:e58371. https://doi.org/10.7554/eLife.58371.
33. Coplen TB. 2011. Guidelines and recommended terms for expression of stable-isotope-ratio and gas-ratio measurement results. Rapid Commun Mass Spectrom 25:2538–2560. https://doi.org/10.1002/rcm.5129.
34. Hayes JM. 1993. Factors controlling ^{13}C contents of sedimentary organic compounds: principles and evidence. Mar Geol 113:111–125. https://doi.org/10.1016/0025-3227(93)90153-M.
35. Childress JJ, Lee RW, Sanders NK, Felbeck H, Oros DR, Toulmond A, Desbruyeres D, Kennicutt MC, Brooks J. 1993. Inorganic carbon uptake in hydrothermal vent tubeworms facilitated by high environmental pCO_2. Nature 362:147–169. https://doi.org/10.1038/362147a0.
36. Fisher CR, Childress JJ, Macko SA, Brooks JM. 1994. Nutritional interactions in Galapagos Rift hydrothermal vent communities: inferences from stable carbon and nitrogen isotope analyses. Mar Ecol Prog Ser 103:45–55. https://doi.org/10.3354/meps103045.
37. Quandt L, Gottschalk G, Ziegler H, Stichler W. 1977. Isotope discrimination by photosynthetic bacteria. FEMS Microbiol Lett 1:125–128. https://doi.org/10.1111/j.1574-6968.1977.tb00596.x.
38. Pardue JW, Scalan RS, Van Baalen C, Parker PL. 1976. Maximum carbon isotope fractionation in photosynthesis by blue-green algae and a green alga. Geochim Cosmochim Acta 40:309–312. https://doi.org/10.1016/0016-7037(76)90208-8.
39. Ruby EG, Jannasch HW, Deuser WG. 1987. Fractionation of stable carbon isotopes during chemoautotrophic growth of sulfur-oxidizing bacteria. Appl Environ Microbiol 53:1940–1943. https://doi.org/10.1128/aem.53.8.1940-1943.1987.
40. Preuß A, Schauder R, Fuchs G, Stichler W. 1989. Carbon isotope fractionation by autotrophic bacteria with three different CO_2 fixation pathways. Z Naturforsch C 44:397. https://doi.org/10.1515/znc-1989-5-610.
41. Madigan MT, Takigiku R, Lee RG, Gest H, Hayes JM. 1989. Carbon isotope fractionation by thermophilic phototrophic sulfur bacteria: evidence for autotrophic growth in natural populations. Appl Environ Microbiol 55:639–644. https://doi.org/10.1128/aem.55.3.639-644.1989.
42. Wirsen CO, Sievert SM, Cavanaugh CM, Molyneaux SJ, Ahmad A, Taylor LT, DeLong EF, Taylor CD. 2002. Characterization of an autotrophic sulfide-oxidizing marine *Arcobacter* sp. that produces filamentous sulfur. Appl Environ Microbiol 68:316–325. https://doi.org/10.1128/AEM.68.1.316-325.2002.
43. House CH, Schopf JW, Stetter KO. 2003. Carbon isotopic fractionation by archaeans and other thermophilic prokaryotes. Org Geochem 34:345–356. https://doi.org/10.1016/S0146-6380(02)00237-1.
44. Fisher CR, Kennicutt MC, Brooks JM. 1990. Stable carbon isotope evidence for carbon limitation in hydrothermal vent vestimentiferans. Science 247:1094–1096. https://doi.org/10.1126/science.247.4946.1094.
45. Melzer E, Schmidt HL. 1987. Carbon isotope effects on the pyruvate dehydrogenase reaction and their importance for relative carbon-13 depletion in lipids. J Biol Chem 262:8159–8164. https://doi.org/10.1016/S0021-9258(18)47543-6.
46. Hayes JM. 2001. Fractionation of carbon and hydrogen isotopes in biosynthetic processes, p 225–277. *In* Valley JW, Cole DR (ed), Stable isotope geochemistry. Mineral Society of America, Washington, DC.
47. Goffredi SK, Childress JJ, Desaulniers NT, Lallier FH. 1997. Sulfide acquisition by the hydrothermal vent tubeworm *Riftia pachyptila* appears to be *via* uptake of HS^-, rather than H_2S. J Exp Biol 200:2609–2616. https://doi.org/10.1242/jeb.200.20.2609.
48. Scott KM, Fisher CR, Vodenichar JS, Nix ER, Minnich E. 1994. Inorganic carbon and temperate requirements for autotrophic carbon fixation by the chemoautotrophic symbionts of the giant hydrothermal vent tube worm, *Riftia pachyptila*. Physiol Zool 67:617–638. https://doi.org/10.1086/physzool.67.3.30163761.
49. Williams CA, Nelson DC, Farah BA, Jannasch HW, Shively JM. 1988. Ribulose bisphosphate carboxylase of the procaryotic symbiont of a hydrothermal vent tube worm: kinetics, activity and gene hybridization. FEMS Microbiol Lett 50:107–112. https://doi.org/10.1111/j.1574-6968.1988.tb02920.x.
50. Scott KM, Boller AJ, Dobrinski KP, Le Bris N. 2012. Response of hydrothermal vent vestimentiferan *Riftia pachyptila* to differences in habitat chemistry. Mar Biol 159:435–442. https://doi.org/10.1007/s00227-011-1821-5.
51. Fisher CR, Childress JJ, Brooks JM. 1988. Are hydrothermal vent vestimentifera carbon limited? Am Zool 28:128.
52. Chypre M, Zaidi N, Smans K. 2012. ATP-citrate lyase: a mini-review. Biochem Biophys Res Commun 422:1–4. https://doi.org/10.1016/j.bbrc.2012.04.144.
53. Yamamoto M, Arai H, Ishii M, Igarashi Y. 2006. Role of two 2-oxoglutarate: ferredoxin oxidoreductases in *Hydrogenobacter thermophilus* under aerobic and anaerobic conditions. FEMS Microbiol Lett 263:189–193. https://doi.org/10.1111/j.1574-6968.2006.00415.x.
54. Mitchell J, Leonard J, Delaney J, Girguis P, Scott K. 2019. Hydrogen does not appear to be a major electron donor for the deep-sea hydrothermal vent symbiosis *Riftia pachyptila*. Appl Environ Microbiol 86:e01522-19. https://doi.org/10.1128/AEM.01522-19.

55. Mall A, Sobotta J, Huber C, Tschirner C, Kowarschik S, Bačnik K, Mergelsberg M, Boll M, Hügler M, Eisenreich W, Berg IA. 2018. Reversibility of citrate synthase allows autotrophic growth of a thermophilic bacterium. Science 359:563–567. https://doi.org/10.1126/science.aao2410.
56. Nunoura T, Chikaraishi Y, Izaki R, Suwa T, Sato T, Harada T, Mori K, Kato Y, Miyazaki M, Shimamura S, Yanagawa K, Shuto A, Ohkouchi N, Fujita N, Takaki Y, Atomi H, Takai K. 2018. A primordial and reversible TCA cycle in a facultatively chemolithoautotrophic thermophile. Science 359:559–563. https://doi.org/10.1126/science.aao3407.
57. Steffens L, Pettinato E, Steiner TM, Mall A, König S, Eisenreich W, Berg IA. 2021. High CO2 levels drive the TCA cycle backwards towards autotrophy. Nature 592:784–788. doi:10.1038/s41586-021-03456–9. https://doi.org/10.1038/s41586-021-03456-9.
58. Dobrinski KP, Longo DL, Scott KM. 2005. A hydrothermal vent chemolithoautotroph with a carbon concentrating mechanism. J Bacteriol 187:5761–5766. https://doi.org/10.1128/JB.187.16.5761-5766.2005.
59. Grassineau NV, Mattey DP, Lowry D. 2001. Sulfur isotope analysis of sulfide and sulfate minerals by continuous flow-isotope ratio mass spectrometry. Anal Chem 73:220–225. https://doi.org/10.1021/ac000550f.
60. Scott KM, Bright M, Macko SA, Fisher CR. 1999. Carbon dioxide use with different affinities by chemoautotrophic endosymbionts of the hydrothermal vent vestimeniferans *Riftia pachyptila* and *Ridgeia piscesae*. Mar Biol 135:25–34. https://doi.org/10.1007/s002270050597.
61. Williams TJ, Zhang CL, Scott JH, Bazylinski DA. 2006. Evidence for autotrophy via the reverse tricarboxylic acid cycle in the marine magnetotactic coccus strain MC-1. Appl Environ Microbiol 72:1322–1329. https://doi.org/10.1128/AEM.72.2.1322-1329.2006.
62. Hügler M, Huber H, Molyneaux SJ, Vetriani C, Sievert SM. 2007. Autotrophic CO_2 fixation via the reductive tricarboxylic acid cycle in different lineages within the phylum *Aquificae*: evidence for two ways of citrate cleavage. Environ Microbiol 9:81–92. https://doi.org/10.1111/j.1462-2920.2006.01118.x.
63. Wahlund TM, Tabita FR. 1997. The reductive tricarboxylic acid cycle of carbon dioxide assimilation: initial studies and purification of ATP-citrate lyase from the green sulfur bacterium *Chlorobium tepidum*. J Bacteriol 179:4859–4867. https://doi.org/10.1128/jb.179.15.4859-4867.1997.
64. Kanao T, Fukui T, Atomi H, Imanaka T. 2001. ATP-citrate lyase from the green sulfur bacterium *Chlorobium limicola* is a heteromeric enzyme composed of two distinct gene products. Eur J Biochem 268:1670–1678. https://doi.org/10.1046/j.1432-1327.2001.02034.x.
65. Schwedock J, Harmer TL, Scott KM, Hektor HJ, Seitz AP, Fontana MC, Distel DL, Cavanaugh CM. 2004. Characterization and expression of genes from the RubisCO gene cluster of the chemoautotrophic symbiont of *Solemya velum*: *cbbLSQO*. Arch Microbiol 182:18–29. https://doi.org/10.1007/s00203-004-0689-x.
66. Fisher CR, Childress JJ, Sanders NK. 1988. The role of vestimentiferan hemoglobin in providing an environment suitable for chemoautotrophic sulfide-oxidizing endosymbionts. Symbiosis 5:229–246.
67. Werner RA, Bruch BA, Brand WA. 1999. ConFlo III—an interface for high precision $\delta^{13}C$ and $\delta^{15}N$ analysis with an extended dynamic range. Rapid Commun Mass Spectrom 13:1237–1241. https://doi.org/10.1002/(SICI)1097-0231(19990715)13:13<1237::AID-RCM633>3.0.CO;2-C.
68. Werner RA, Brand WA. 2001. Referencing strategies and techniques in stable isotope ratio analysis. Rapid Commun Mass Spectrom 15:501–519. https://doi.org/10.1002/rcm.258.
69. Qi H, Coplen TB, Geilmann H, Brand WA, Bohlke JK. 2003. Two new organic reference materials for $\delta^{13}C$ and $\delta^{15}N$ measurements and a new value for the $\delta^{13}C$ of NBS 22 oil. Rapid Commun Mass Spectrom 17:2483–2487. https://doi.org/10.1002/rcm.1219.
70. Coplen TB, Brand WA, Gehre M, Gröning M, Meijer HAJ, Toman B, Verkouteren RM. 2006. New guidelines for $\delta^{13}C$ measurements. Anal Chem 78:2439–2441. https://doi.org/10.1021/ac052027c.
71. Hanson TE, Tabita FR. 2001. A ribulose 1,5-bisphosphate carboxylase/oxygenase (RubisCO)-like protein from *Chlorobium tepidum* that is involved with sulfur metabolism and the response to oxidative stress. Proc Natl Acad Sci U S A 98:4397–4402. https://doi.org/10.1073/pnas.081610398.
72. Scott KM, Sievert SM, Abril FN, Ball LA, Barrett CJ, Blake RA, Boller AJ, Chain PS, Clark JA, Davis CR, Detter C, Do KF, Dobrinski KP, Faza BI, Fitzpatrick KA, Freyermuth SK, Harmer TL, Hauser LJ, Hügler M, Kerfeld CA, Klotz MG, Kong WW, Land M, Lapidus A, Larimer FW, Longo DL, Lucas S, Malfatti SA, Massey SE, Martin DD, McCuddin Z, Meyer F, Moore JL, Ocampo LH, Paul JH, Paulsen IT, Reep DK, Ren Q, Ross RL, Sato PY, Thomas P, Tinkham LE, Zeruth GT. 2006. The genome of deep-sea vent chemolithoautotroph *Thiomicrospira crunogena*. PLoS Biol 4:e383-17. https://doi.org/10.1371/journal.pbio.0040383.
73. Rodríguez-Ruiz J, Belarbi E-H, Sánchez JLG, Alonso DL. 1998. Rapid simultaneous lipid extraction and transesterification for fatty acid analyses. Biotechnol Tech 12:689–691. https://doi.org/10.1023/A:1008812904017.
74. Ott L. 1988. An introduction to statistical methods and data analysis. PWS-Kent Publishing Company, Boston, MA.
75. Sakata S, Hayes JM, McTaggart AR, Evans RA, Leckrone KJ, Togasaki RK. 1997. Carbon isotopic fractionation associated with lipid biosynthesis by a cyanobacterium: relevance for interpretation of biomarker records. Geochim Cosmochim Acta 61:5379–5389. https://doi.org/10.1016/s0016-7037(97)00314-1.
76. Sakata S, Hayes JM, Rohmer M, Hooper AB, Seemann M. 2008. Stable carbon-isotopic compositions of lipids isolated from the ammonia-oxidizing chemoautotroph *Nitrosomonas europaea*. Org Geochem 39:1725–1734. https://doi.org/10.1016/j.orggeochem.2008.08.005.
77. van der Meer MTJ, Schouten S, Sinninghe Damsté JS. 1998. The effect of the reversed tricarboxylic acid cycle on the ^{13}C contents of bacterial lipids. Org Geochem 28:527–533. https://doi.org/10.1016/S0146-6380(98)00024-2.